PRESCRIBED PERFORMANCE CONTROL OF UNDERACTUATED SURFACE VESSELS' TRAJECTORY USING A NEURAL NETWORK AND INTEGRAL TIME-DELAY SLIDING MODE

Yun Chen and Hua Chen

To tackle the underactuated surface vessel (USV) trajectory tracking challenge with input delays and composite disturbances, an integral time-delay sliding mode controller based on backstepping is discussed. First, the law of virtual velocity control is established by coordinate transformation and the position error is caused to converge utilizing the performance function. At the same time, based on the estimation of velocity vector by the high-gain observer (HGO), radial basis function (RBF) neural network is applied to compensate for both the uncertainty of model parameters and external disturbances. The longitudinal and heading control laws are presented in combination with the integral time-delay sliding mode control. Then, on the basis of Lyapunov - Krasovskii functional and stability proof, virtual velocity error is guaranteed to converge to 0 in finite time. Finally, the outcomes of the numerical simulation demonstrate the reliability and efficiency of the proposed approach.

Keywords: underactuated surface vessels, trajectory tracking, time-delay, external disturbances, sliding mode, backstepping, radial basis function(RBF)

Classification: 93A30, 93Dxx

1. INTRODUCTION

Considering the safety of human operation in the marine environment and the economy of marine equipment, the application and development of underactuated surface vessels(USVs) is of great significance. USV has a wide range of applications, including marine oil and gas exploration, oceanographic mapping, coastal surveillance, etc. [9, 18]. Due to the uncertainty and complexity of the marine environment, the key technology for USV to achieve autonomous navigation is the reliability, stability and accuracy of trajectory tracking control [15]. Different from path tracking, trajectory tracking requires the vessel to track time-varying trajectory on time and has strict requirements on velocity and time [16]. However, actuator delays will cause control force and torque delays in the specific implementation of the USV, which will impact the reliability of the system. Consequently, the concern of input delay becomes one of the main points of this paper. Meanwhile, due to nonlinear dynamics with high coupling and time-varying

disturbances constraints of ocean currents [10], accurate model parameters cannot be obtained. Hence, delays, imprecise constraints, and disturbances bring challenges to USV controller design and system stability.

The common methods of trajectory tracking control are multivariable model decoupling and system local linearization. For the problem of trajectory tracking caused by external disturbances and model parameter uncertainty, Lyapunov control, output feedback control, backstepping control and sliding mode control are mainly adopted at present [4, 13]. A single control mechanism typically has shortcomings, though. An trouble with backstepping control is that it needs to calculate the derivatives of virtual variables for many times, the calculation process is complicated, and the vehicle needs to provide sufficient acceleration, which is difficult to achieve in practice. Although the sliding mode method has the advantages of fast response and insensitivity to parameters and disturbances change, the chattering phenomenon always exists in the sliding mode control, which will cause the wear of the actuator cite2020Overview. In recent years, compound control has attracted more and more attention. In [14], An adaptive backstepping controller is mentioned to estimate the entire nonlinear damping and disturbances simultaneously without accurately knowing the parameter vector dimension of model uncertainty. Zou et al. used RBF neural network to estimate the model parameter uncertainty, and adopted backstepping control and predefined performance functions to converge the tracking error [28]. Similarly, Qiu et al. constructed a radial basis neural network using the minimum learning parameter(MLP) method to approach the uncertain system dynamics online [20]. Unfortunately, it is challenging for the forward neural network to represent the impact of time series of input and output elements, and it takes a long time for trajectory transition when trajectory mutation occurs. In [24], external disturbances are observed by nonlinear disturbance observer. Yao designed fixed-time sliding mode control has strong robustness to centralized uncertainties [19]. Nevertheless, the controller proposed in [19] requires a known upper bound of centralized uncertainties, which is difficult to realize in practice. Meanwhile, due to the variability and abruptness of the marine working environment, it is impossible to measure the vehicle velocity once the sensor fails. Therefore, this paper estimates the velocity with a high-gain observer.

In actual marine operations, the movement of USV is operated by a controlled voltage signal that serves as the control input to the actuator. As the control force, control voltage and velocity of USV are in a complex nonlinear mapping relationship [1], the input delay of actuators will lead to hysteretic changes in position and attitude of the USV. Therefore, in the actual USV controller design process, directly ignoring the time delay will generate the increase of system overshoot [26] and the decrease of trajectory tracking control accuracy. Based on the above analysis, time delays are added into the controller design of the USV to improve the stability and reliability of trajectory tracking. Lakhekar et al. adopted time delay estimator(TDE) to identify unknown nonlinear dynamics and perturbations through state derivatives and each delay information of control inputs [11]. In [8], Feng et al. partitioned the delay interval into multiple nonuniform subintervals to study the stability of continuous time-delay systems. Aiming at the problem of input time delay, Zhou et al. realized synchronous tracking of the desired trajectory by establishing a state predictor [27]. Druzhinina et al. proposed

convex optimization problems for the system with feedback delays, states, and control constraints to obtain estimates of control parameters and initial condition domains [6]. Although there are many researches on the stability of systems with time delays, the researches on USV trajectory tracking control with time delays are few.

Motivated by the above discussion, the trajectory tracking problem of USV with delays and external disturbances is studied in this paper. Inspired by the RBF algorithm for autonomous underwater vehicles(AUVs) in [27], nonlinear terms with unknown disturbances and model parameter uncertainty are estimated with fewer adjustment parameters. Different from [5, 21], the former does not consider chattering of sliding mode while combining neural network and sliding control method. In this paper, saturation function is used in sliding mode control to reduce chattering. Combined with coordinate transformation, we propose an integral time-delay sliding mode control (ITDSMC) method based on backstepping. The following is a summary of this paper's significant contributions:

1. ITDSMC based on backstepping and Barbalat's lemma guarantees the position and velocity error convergence and the stability of the system.

2. For the model parameter uncertainty and external disturbances of the USV, RBF neural network and HGO are adopted to estimate the velocity vector and composite disturbances. Compared with other control schemes based on neural network approximation techniques, this paper approximates the centralized uncertainties with fewer parameters and has strong robustness.

3. According to the performance requirements and constraints of the system, ensure that the position tracking error enters and remains within the preset steady-state error band.

The remainder of this essay is structured as follows. The kinematic and dynamic models of USV are described in section 2 and the trajectory tracking error equations are established. The ITDSMC controller is designed in section 3. The stability of the pertinent closed-loop tracking error system is examined in section 4. Section 5 displays the simulations and correlation analysis. Finally, section 6 summarizes this paper.

2. PROBLEM STATEMENT

In this section, kinematic and dynamic models of underactuated surface vessels with input delays and uncertain model parameters are proposed. Then, for simplicity, the internal and external disturbances are regarded as composite disturbances to simplify the dynamic model. The desired position vector's kinematic model is then established. Enabling the underactuated surface vessel track the appropriate location and velocity is the goal of this work.

2.1. USV 3-degree-of-freedom(DOF) mathematical model

Different from the general 6-DOF USV model, this paper simplified the USV into a 3-DOF model was used under the supposition that heave, roll, and pitch motions were ignored, and the actuators' generated surge force and yaw moment functioned as the

reduced order model's control input (propeller and rudder)[12]. In addition, the earth-fixed frame (E) and the body-fixed frame (B) are defined for motion and force analysis of the USV, as shown in Figure 1.
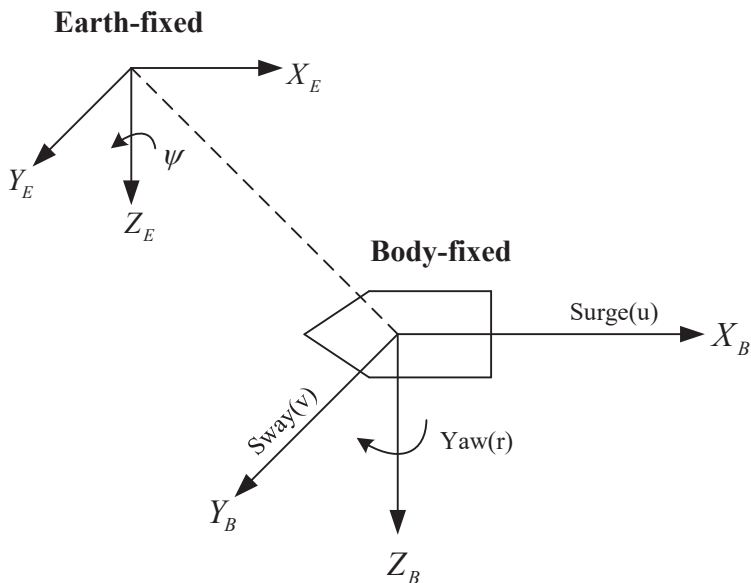
Fig. 1. Body-fixed frame and earth-fixed reference frame for USV.

This paper considers that the USV is symmetric in XOY, YOZ and XOZ planes, so the influence of off-diagonal terms of inertia matrix M and damping matrix D is neglected. The matrix vectors for the mathematical model of the kinematic and dynamic of the horizontal USV are described as:

$$\begin{cases} \dot{\eta} = J(\psi)\nu \\ M\dot{\nu} = -C(\nu)\nu - D(\nu)\nu + \tau_\omega + \tau_c(t-T) + \delta \end{cases} \tag{1}$$

where $J(\psi) = \begin{bmatrix} \cos\psi & -\sin\psi & 0 \\ \sin\psi & \cos\psi & 0 \\ 0 & 0 & 1 \end{bmatrix}$, $M = \begin{bmatrix} m_{11} & 0 & 0 \\ 0 & m_{22} & 0 \\ 0 & 0 & m_{33} \end{bmatrix}$,

$C(\nu) = \begin{bmatrix} 0 & 0 & -m_{22}\upsilon \\ 0 & 0 & m_{11}u \\ m_{22}\upsilon & -m_{11}u & 0 \end{bmatrix}$, $D(\nu) = \begin{bmatrix} d_{11} & 0 & 0 \\ 0 & d_{22} & 0 \\ 0 & 0 & d_{33} \end{bmatrix}$,

where $\eta = [x, y, \psi]^T$ depicts the USV's position and orientation in the earth-fixed frame, $J(\eta)$ denotes the matrix of change from the body-fixed frame to the earth-fixed frame, $\nu = [u, \upsilon, r]^T$ represents the velocity vectors in the body-fixed frame, M denotes the inertia matrix, which contains additional mass terms, $C(\nu)$ is the Centripetal and Coriolis forces matrix, $D(\nu)$ is the hydrodynamic damping matrix, $\tau_\omega = [\tau_{\omega u}, \tau_{\omega v}, \tau_{\omega r}]^T$ denotes

the external time-varying disturbance, $\tau_c(t - T) = [\tau_u(t - T), 0, \tau_r(t - T)]^T$ denotes control input of the system, $\delta = [\delta_u, \delta_v, \delta_r]^T$ denotes the vector of uncertain model parameters, often known as the "internal disturbance." To facilitate processing, internal disturbance τ_ω and external disturbance δ are combined into composite disturbances, that is, $d = \tau_\omega + \delta$. Rewriting the equation (1) as:

$$\begin{cases} \dot{\eta} = J(\psi)\nu \\ M\dot{\nu} = -C(\nu)\nu - D(\nu)\nu + \tau_c(t - T) + d \end{cases} \tag{2}$$

where $d = [d_u, d_v, d_r]^T$, $T \in R^+$ represents bounded input delay constant, satisfying $T \leq \bar{T}$, $\bar{T}$ is the upper bound.

By expanding the matrix form of equation (2), the USV's dynamic and kinematic models are developed as [26]:

$$\begin{cases} \dot{x} = u \cos \psi - \upsilon \sin \psi \\ \dot{y} = u \sin \psi + \upsilon \cos \psi \\ \dot{\psi} = r \end{cases} \tag{3}$$

$$\begin{cases} \dot{u} = \frac{m_{22}}{m_{11}} \upsilon r - \frac{d_{11}}{m_{11}} u + \frac{1}{m_{11}} \tau_u(t - T) + \frac{d_u}{m_{11}} \\ \dot{\upsilon} = -\frac{m_{11}}{m_{22}} ur - \frac{d_{22}}{m_{22}} \upsilon + \frac{d_v}{m_{22}} \\ \dot{r} = \frac{m_{11} - m_{22}}{m_{33}} u\upsilon - \frac{d_{33}}{m_{33}} r + \frac{1}{m_{33}} \tau_r(t - T) + \frac{d_r}{m_{33}} \end{cases} \tag{4}$$

where $m_{11} = m - X_{\dot{u}}$, $m_{22} = m - Y_{\dot{v}}$, $m_{33} = I_z - N_{\dot{r}}$, $d_{11} = X_u + X_{u|u|}|u|$, $d_{22} = Y_v + Y_{v|v|}|\upsilon|$, $d_{33} = N_r + N_{r|r|}|r|$, where I_z is the component of the moment of inertia, $X_{\dot{u}}, Y_{\dot{v}}, N_{\dot{r}}, X_u, X_{u|u|}, Y_v, Y_{v|v|}, N_r, N_{r|r|}$ are hydrodynamic damping coefficients.

To make the design process simpler, the nonlinear system studied in this paper satisfies the following assumptions [3, 26, 27]:

Assumption 1. The desired position vector $[x_d, y_d]^T$ is differentiable.

Assumption 2. The USV's control inputs and velocity terms are bounded.

Assumption 3. The external disturbance τ_ω of the USV is time-varying and bounded, that is, satisfying $\|\tau_{\omega u}\| \leq \bar{\tau}_{\omega u}, \|\tau_{\omega v}\| \leq \bar{\tau}_{\omega v}, \|\tau_{\omega r}\| \leq \bar{\tau}_{\omega r}$, where $\bar{\tau}_{\omega u}, \bar{\tau}_{\omega v}, \bar{\tau}_{\omega r}$ are known.

Assumption 4. The parameter perturbations have upper limits.

2.2. USV trajectory tracking error equation model

At first, defining $[x_d, y_d, \psi_d]^T$ as the desired position state vector of the USV at earth-fixed frame. Therefore, the position error variables of the USV are follows:

$$\begin{cases} x_e = x - x_d \\ y_e = y - y_d \end{cases}$$

where $E_1 = [x_e, y_e]^T$.

Through coordinate transformation, the position error variables of USV at body-fixed frame are obtained

$$\begin{bmatrix} e_x \\ e_y \end{bmatrix} = \begin{bmatrix} \cos \psi & \sin \psi \\ -\sin \psi & \cos \psi \end{bmatrix} \begin{bmatrix} x_e \\ y_e \end{bmatrix}, \tag{5}$$

where $E_B = [e_x, e_y]^T$.

To improve USV's performance and capability, the system error enters the preset steady-state error band. The preset performance of USV trajectory tracking control is defined as follows:

$$- \underline{e}_i(t) < e_i(t) < \overline{e}_i(t), \; i = x, y \tag{6}$$

where $\underline{e}_i(t), \overline{e}_i(t)$ are the upper and lower bounds on the preset performance function.

In this paper, the maximum steady state, terminal time and convergence rate are combined to adopt the following performance function [7]

$$\overline{e}_i(t) = \begin{cases} (\overline{e}_{i,0} - \overline{e}_{i,t_f}) \exp(-p_i \frac{t_f t}{t_f - t}) + \overline{e}_{i,t_f}, \; 0 \leq t < t_f \\ \overline{e}_{i,t_f}, \; t \geq t_f \end{cases}$$

$$- \underline{e}_i(t) = \begin{cases} -(\underline{e}_{i,0} - \underline{e}_{i,t_f}) \exp(-p_i \frac{t_f t}{t_f - t}) - \underline{e}_{i,t_f}, \; 0 \leq t < t_f \\ -\underline{e}_{i,t_f}, \; t \geq t_f \end{cases} \tag{7}$$

where $\overline{e}_{i,0}, \underline{e}_{i,0}$ represent the initial values of the performance function, $\overline{e}_{i,t_f}, \underline{e}_{i,t_f}$ are the boundary values of the preset trajectory tracking error band within the predefined time t_f, and p_i is the convergence rate of the performance function.

Remark 1. The proposed new preset performance function Eq.(7) can preset the expected time t_f according to the performance requirements and constraints of the system to ensure that its function value reaches $\overline{e}_{i,t_f} \, and -\underline{e}_{i,t_f}$ respectively at the expected time t_f, so that the controller designed based on this performance function can realize that the position tracking error of the USV enters within the preset expected time t_f and no longer exceeds the preset steady-state error band $[-\underline{e}_{i,t_f}, \overline{e}_{i,t_f}]$.

Deriving equation (5) and substituting equation (3) into it, the USV's error tracking model can be written as:

$$\begin{cases} \dot{e}_x = u - v_p \cos \psi_e + r e_y \\ \dot{e}_y = v + v_p \sin \psi_e - r e_x \end{cases} \tag{8}$$

where $\psi_e = \psi - \psi_d$ denotes the heading angle error of the USV, $\psi_d = \arctan(\dot{x}_d/\dot{y}_d)$, $v_p = \sqrt{\dot{x}_d^2 + \dot{y}_d^2}$ represents the desired heading angle and desired velocity of the USV.

For the convenience of subsequent proof and calculations, we introduce the following lemma.

Lemma 2.1. (Barbalat [17]) For differentiable function $f(t) \in L_\infty, t \geq 0$, its derivative is bounded and $f(t) \in L_p$, where $p \in [1, \infty)$, then $\lim_{t \to \infty} f(t) = 0$.

3. CONTROLLER DESIGN

After establishing the mathematical model of USV, the trajectory control problem is converted into the controller design of the kinematic and dynamic systems. For the kinematic system, virtual velocity control law is designed by backstepping method. In

order to estimate the composite interference and minimize the system's reliance on time delays, the ITDSMC law is devised for the dynamic system, and the RBF neural network algorithm is employed to estimate the composite interference. In summary, the control structure diagram of this paper is shown in Figure 2
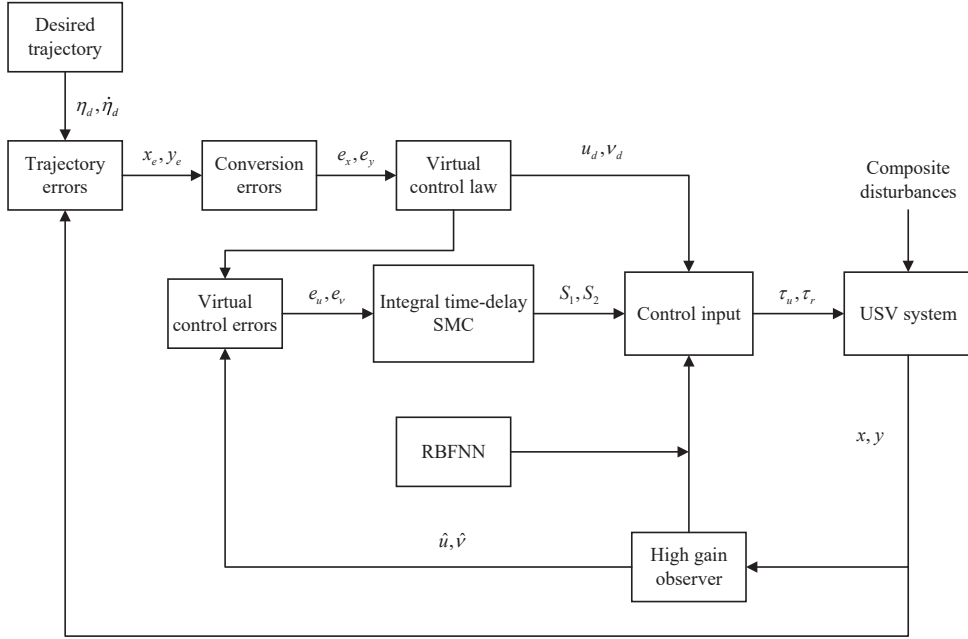

Fig. 2. The structure of the proposed control scheme for the USV.

3.1. Kinematic system control law

Designing the error conversion function as follows:

$$z_i = \frac{\bar{e}_i \underline{e}_i e_i}{(\bar{e}_i - e_i)(e_i + \underline{e}_i)}, \tag{9}$$

where $z_i, i = x, y$ is the converted error.

Deriving z_i and we obtain

$$\dot{z}_i = Q_i \dot{e}_i - R_i, \tag{10}$$

where $Q_i = \dfrac{\bar{e}_i \underline{e}_i e_i^2 + \bar{e}_i^2 \underline{e}_i^2}{(\bar{e}_i - e_i)^2 (e_i + \underline{e}_i)^2}, R_i = \dfrac{e_i^3 (\dot{\bar{e}}_i \underline{e}_i + \bar{e}_i \dot{\underline{e}}_i)}{(\bar{e}_i - e_i)^2 (e_i + \underline{e}_i)^2} + \dfrac{e_i^2 (\dot{\bar{e}}_i \underline{e}_i^2 + \bar{e}_i^2 \dot{\underline{e}}_i)}{(\bar{e}_i - e_i)^2 (e_i + \underline{e}_i)^2}.$

For the surge velocity u and sway velocity v, the following virtual control laws u_d, v_d are designed

$$\begin{bmatrix} u_d \\ v_d \end{bmatrix} = \begin{bmatrix} v_p \cos\psi_e - re_y - Q_x^{-1}(k_1 z_x - R_x) \\ -v_p \sin\psi_e + re_y - Q_y^{-1}(k_2 z_y - R_y) \end{bmatrix}, \tag{11}$$

where $k_1, k_2 > 0$ are adjustable control gains.

While $u_d \to u, v_d \to v$, the equation (8) can be rewritten as

$$\begin{cases} \dot{e}_x = -Q_x^{-1}(k_1 z_x - R_x) \\ \dot{e}_y = -Q_y^{-1}(k_2 z_y - R_y) \end{cases} . \tag{12}$$

Substituting the equation (12) into (10), we have

$$\dot{z}_x = -k_1 z_x, \dot{z}_y = -k_2 z_y. \tag{13}$$

The Lyapunov function is constructed as

$$V_1 = \frac{1}{2} z_x^2 + \frac{1}{2} z_y^2. \tag{14}$$

Substituting (13) into $\dot{V}_1$, we obtain

$$\dot{V}_1 = -k_1 z_x^2 - k_2 z_y^2. \tag{15}$$

It is obvious from equation (15) that $\dot{V}_1 \leq 0$, under circumstance of $u = u_d, v = v_d$, if and only if $(x_e, y_e) = 0, \dot{V} = 0$, the Lyaponov stability theory predicts that x_e, y_e will asymptotically convergence.

3.2. Dynamic system control law

The controller is constructed in four steps in this part. Firstly, RBF neural network is introduced and applied to estimate unknown terms. Then, the dynamic system with time delays is transformed. Finally, the ITDSMC law is designed as the actual control law for the virtual velocity error.

Step 1. As a forward neural network [23], the radial basis function neural network has a mapping between the input and output, nonetheless, there is a linear mapping between the hidden layer and the output, which improves the learning rate. The architecture of RBFNN is shown as Figure 3. As a result, the properties of the RBF are its simple structure, excellent nonlinear approximation ability, and quick convergence rate. Also, it can approximate arbitrary function with arbitrary precision.

For the smooth nonlinear function $f : \Omega \to R$, its neural network output expression is:
$$f = W^{*T} H(x) + \varsigma(x),$$

where $x = [u, v, r]^T \in \Omega$ is the neural network's input, Ω is the compact set on R^n, $W^* \in R^{n \times 1}$ is the optimum neural network weight, $\varsigma(x)$ is the neural network's approximation error, satisfying $\|\varsigma\| \leq \bar{\varsigma}, \bar{\varsigma} > 0$. $H(x) \in R^{n \times 1}$ is the neural network's radial basis function vector, $h_n(x)$ is the Gaussian basis function output, which is selected as follows:

$$h_j(x) = \exp\left(\frac{\|x - c_j\|}{2b_j^2} \right), \ (j = 1, 2, \ldots, n), \tag{16}$$

where j is the jth node of the neural network's hidden layer, c_j is the center point vector of neuron in jth hidden layer.
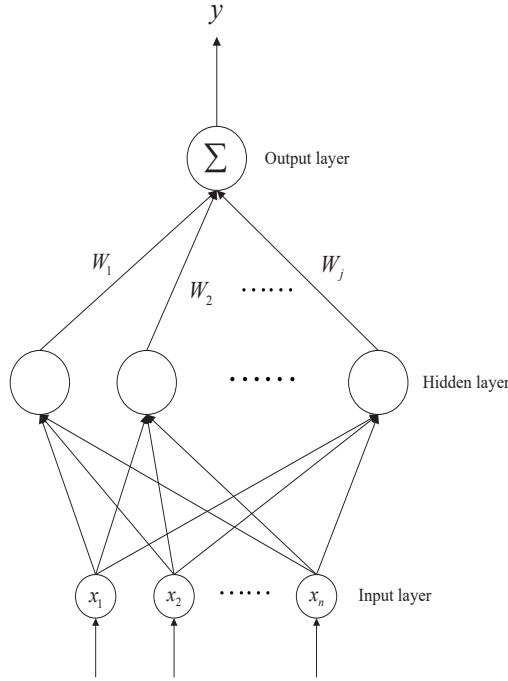
Fig. 3. The architecture of RBF neural network.

Regarding the Gaussian function (16), we introduce the following important lemma.

Lemma 3.1. (Guoqing et al. [25]) For the Gaussian function (16), if $\hat{x} = x - g\bar{\psi}$, where $g > 0$ is a constant and $\bar{\psi}$ is a bounded vector, that is, $|\bar{\psi}_k| \leq b_k, b_k > 0, k = 1, \ldots, n$ for all $t > t^* > 0$. Then, we obtain

$$H(\hat{x}) = H(x) - gI_t, \tag{17}$$

where I_t is a bounded vector.

Assuming $\|W^*\| \leq \bar{W}, \bar{W} \in R^+$ is the upper bounded. The estimated value of W^* that minimizes $\varsigma(x)$ in compact set Ω, is defined as:

$$W^* \triangleq \arg \min_{W \in R^n} \{\sup_{x \in \Omega} |\hat{W}^T H(x) - f|\}.$$

Since the ideal weight value W^* is often difficult to obtain in practice, $\hat{W} \in R^{n \times 1}$ is used to represent its estimated value, and $\tilde{W}$ is the estimated error, satisfying $\tilde{W} = \hat{W} - W^*$. Consequently, the following is the estimates of the unknown nonlinear term:

$$\hat{f} = W^T H(x). \tag{18}$$

The RBF neural network's weight adaptive law is designed as

$$\dot{\hat{W}} = \Gamma[S^T H(\hat{x}) + \mu \hat{W} + \varrho S^T I_t],$$ (19)

where Γ, μ are the design constants to be selected, S is the sliding surface.

Step 2. Considering that the velocity of USV may be unmeasurable, to estimate the vehicle velocity with composite disturbances, we use a high gain observer, and introduce the following lemma.

Lemma 3.2. (Behtash [2]) For the liner system (20)

$$\begin{cases} \varrho \dot{\xi}_k = \xi_{k+1}, k = 1, \dots, n-1 \\ \varrho \dot{\xi}_n = -\bar{w}_1 \xi_n - \dots - \bar{w}_{n-1} \xi_2 - \xi_1 + \eta(t) \end{cases}$$ (20)

where $\eta(t)$ is the system's output vector, ξ_k are the HGO's state variables, and $\varrho > 0$ is a tiny constant. The parameters $\bar{w}_k, k = 1, \dots, n-1$ can fulfill the polynomial $s^n + \bar{w}_1 s^{n-1} + \dots + \bar{w}_{n-1} s + 1$ being Hurwitz.

Assuming that $\eta(t)$ is bounded and $|\eta^{(k)}| < M_k, k = 0, \dots, n-1$, where $k = 0, \dots, n-1$ are the first order to the $(n-1)th$ derivatives, then it holds

$$\frac{\xi_{k+1}}{\varrho_k} - \eta_{(k)} = -\varrho \bar{\psi}^{(k+1)}, k = 0, \dots, n-1,$$ (21)

where $\bar{\psi} = \xi_n + \bar{w}_1 \xi_{n-1} + \dots + \bar{w}_{n-1} \xi_1$.

Next, the high gain observer of USV system is constructed. In practice, both the output vector and its first derivative have limited bounds. Taking the following linear system into account

$$\begin{cases} \varrho \dot{\xi}_1 = \xi_2, \\ \varrho \dot{\xi}_2 = -\varpi_1 \xi_2 - \xi_1 + \eta, \end{cases}$$ (22)

where ϖ_1 is positive constant. Therefore, $\hat{\eta} = \pi_2/\varrho$ may be used to calculate the estimate of $\dot{\eta}$, substituting it into equation (1), we obtain

$$\hat{\nu} = J^T(\psi)(\frac{\pi_2}{\varrho}).$$ (23)

According to Lemma 3, then the following property holds

$$\hat{\nu} - \nu = J^T(\psi)(\frac{\pi_2}{\varrho} - \dot{\eta}) = -\varrho J^T(\psi)\bar{\psi}^{(2)}.$$ (24)

Taking the norm of both sides and substituting $\|J^T(\psi)\| = 1$ into it, we have

$$\|\hat{\nu} - \nu\| = \varrho\|\bar{\psi}^{(2)}\| \leq \varrho b_\nu,$$ (25)

where $b_\nu > 0$ is a constat.

Step 3. The first-order nonlinear sliding surface is defined as follows:

$$S_1 = e_u + \lambda_1 \int_0^t e_u(l) \, \mathrm{d}l, \tag{26}$$

where $\lambda_1 > 0$ is constant.

Derived from equation (26) and referencing [3]:

$$\begin{aligned}\dot{S}_1 &= \dot{e_u} + \lambda_1 e_u \\ &= \frac{m_{22}}{m_{11}} v(t - T) r(t - T) - \frac{d_{11}}{m_{11}} u(t - T) + \frac{1}{m_{11}} \tau_u - \dot{u}_d + \lambda_1 e_u + \frac{d_u}{m_{11}},\end{aligned} \tag{27}$$

substituting $\omega_1 = \frac{d_u}{m_{11}}$, $\hat{\kappa} = \frac{\hat{m}_{22}}{\hat{m}_{11}} v(t - T) r(t - T) - \frac{\hat{d}_{11}}{\hat{m}_{11}} u(t - T) - \dot{u}_d + \lambda_1 e_u$ into $\dot{S}_1$:

$$\dot{S}_1 = \frac{\tau_u}{m_{11}} + \hat{\kappa} + \omega_1. \tag{28}$$

Chattering caused by sliding mode prevents continuous USV operation in practical engineering applications. The below saturation function is implemented to lessen the chattering impact of sliding mode:

$$sat(S_i/\Delta) = \begin{cases} 1, & S_i > \Delta_i \\ S_i/\Delta, & |S_i/\Delta| \leq 1 \\ -1, & S_i < \Delta_i \end{cases}, \tag{29}$$

where Δ_i is a smaller positive constant. establishing an arbitrarily thin boundary layer around S_i.

Considering the parameter uncertainty of equation (27), the system's constant velocity approximation law is intended to eliminate the detrimental effect.

$$\beta_1 = \frac{\tilde{m}_{22}}{\tilde{m}_{11}} |v(t - T) r(t - T)| - \frac{\tilde{d}_{11}}{\tilde{m}_{11}} |u(t - T)| - |\dot{u}_d| + \lambda_1 |e_u| + \rho_1, \tag{30}$$

where $\rho_1 > 0$ is the design constant.

According to the design principle of sliding mode control method and in combination with (28) and (30), the design of the longitudinal control legislation is as follows:

$$\tau_u = m_{11}[-\hat{\kappa} - \beta_1 sat(S_1/\Delta_1) - A_1 S_1 - G_1 S_1(t - \bar{T}) - \hat{\omega}_1 - \varepsilon(S_1^T)^{-1} \bar{W}_1^2], \tag{31}$$

where $A_1 > 0$, The gain factor matrix to be chosen is represented by $G_1.$, $\hat{\omega}_1$ is the estimated value of ω_1, $\varepsilon \geq \mu$ is the positive constant, and $\bar{W}_1 \geq \|W_1^*\|$ is the upper bound of W_1^*.

Step 4. For virtual velocity error e_v, the second-order nonlinear sliding surface shown below is established:

$$S_2 = \dot{e}_v + 2\lambda_2 e_v + \lambda_2^2 \int_0^t e_v \, \mathrm{d}l, \tag{32}$$

where λ_2 is positive constant.

Derived from equation (32):

$$\dot{S}_2 = \ddot{e}_v + 2\lambda_2\dot{e}_v + \lambda_2^2 e_v. \tag{33}$$

The derivatives of equation (10) can be obtained:

$$\begin{aligned}
\ddot{e}_v &= -\frac{m_{11}}{m_{22}m_{33}}u(t-T)[(m_{11}-m_{22})v(t-T)u(t-T) - d_{33}r(t-T) \\
&\quad + \tau_r + d_r] - \frac{m_{11}}{m_{22}}\dot{u}r(t-T) - \frac{d_{22}}{m_{22}}\dot{v} + \frac{1}{m_{22}}\dot{d}_v - \ddot{v}_d,
\end{aligned} \tag{34}$$

Substituting equation (34) into equation (33) to obtain:

$$\dot{S}_2 = \frac{o}{m_{22}m_{33}}\tau_r - \frac{\hat{\iota}}{m_{22}m_{33}} + \omega_2, \tag{35}$$

where $o = -m_{11}(e_u + u_d), \omega_2 = -\frac{m_{11}}{m_{22}m_{33}}u(t-T)d_r + \frac{1}{m_{22}}\dot{d}_v$ and

$$\begin{aligned}
\hat{\iota} &= -\hat{m}_{11}(e_u + u_d)[(\hat{m}_{11}-\hat{m}_{22})u(t-T)v(t-T) - \hat{d}_{33}r(t-T)] \\
&\quad - \hat{m}_{11}\hat{m}_{33}\dot{u}r(t-T) - \hat{m}_{33}\hat{d}_{22}\dot{v}.
\end{aligned}$$

Similar to Step 3, to counteract the detrimental impacts of parameter uncertainty, the constant velocity approximation law β_2 is established.

$$\beta_2 = \frac{\tilde{\iota}}{\tilde{m}_{22}\tilde{m}_{33}} + \rho_2, \tag{36}$$

where $\rho_2 > 0$ is the design constant to be determined.

Combined with equation (35), the design of the heading control law is as follows:

$$\begin{aligned}
\tau_r &= \frac{\hat{m}_{22}\hat{m}_{33}}{\hat{o}}[\frac{\hat{\iota}}{\hat{m}_{22}\hat{m}_{33}} - \beta_2 sat(S_2/\Delta_2) - A_2 S_2 \\
&\quad - G_2 S_2(t-\bar{T}) - \hat{\omega}_2 - \varepsilon(S_2^T)^{-1}\bar{W}_2^2],
\end{aligned} \tag{37}$$

where A_2 is the positive constant and G_2 is the gain coefficient matrix to be selected, $\hat{\omega}_2$ is the estimated value of ω_2, and $\bar{W}_2 \geq \|W_2^*\|$ is the upper bound of W_2^*.

4. STABILITY ANALYSIS

In this section, the time-varying disturbances term is estimated by RBF neural network and ITDSMC law for the trajectory tracking control law with input delays.

Theorem 1. For the underactuated surface vessel (USV) trajectory tracking system (2) with time delays and composite time-varying disturbances, on condition that the USV's kinematic model (3) and dynamic model (4) meet the Assumption 1-4, adopting the integral sliding surface which is designed by (26) and (32), and the corresponding virtual velocity control laws depicted in (31) and (37),the system is finally uniformly bounded stable and the desired nonlinear sliding surface converges.

Selecting the following Lyapunov - Krasovskii function with time-delay integral term:

$$V_2 = \frac{1}{2}S_1^T S_1 + \frac{1}{2}\Gamma_1^{-1}\tilde{W}_1^T\tilde{W}_1 + \int_{t-\bar{T}}^{t} S_1^T P_1 S_1 \, \mathrm{d}\sigma + \frac{1}{2}S_2^T S_2 + \frac{1}{2}\Gamma_2^{-1}\tilde{W}_2^T\tilde{W}_2 + \int_{t-\bar{T}}^{t} S_2^T P_2 S_2 \, \mathrm{d}\sigma,$$

(38)

where $P = diag(P_1, P_2)$ is positive matrix, it is obvious from equation (38) that $V \geq 0$. The derivative of the above formula is:

$$\dot{V}_2 = S_1^T\dot{S}_1 + \Gamma_1^{-1}\tilde{W}_1^T\dot{\tilde{W}}_1 + S_1^T(t-\bar{T})P_1 S_1(t-\bar{T}) + S_2^T\dot{S}_2 + \Gamma_2^{-1}\tilde{W}_2^T\dot{\tilde{W}}_2 + S_2^T(t-\bar{T})P_2 S_2(t-\bar{T}).$$

(39)

From $\tilde{W}_i = \hat{W}_i - W_i^*, i = 1, 2$ and the designed controller (28), (31), (35), (37), we obtain:

$$\begin{aligned}
\dot{V}_2 =& S_1^T[-\beta_1 sat(S_1/\Delta_1) - A_1 S_1 - G_1 S_1(t - \bar{T}) + \tilde{\omega}_1 - \varepsilon_1(S_1^T)^{-1}\bar{W}_1^2] - \Gamma_1^{-1}\tilde{W}_1^T\dot{\hat{W}}_1 \\
&+ S_1^T P_1 S_1 + S_1^T(t - \bar{T})P_1 S_1(t - \bar{T}) + S_2^T[-\beta_2 sat(S_2/\Delta_2) - A_2 S_2 - G_2 S_2(t - \bar{T}) \\
&+ \tilde{\omega}_2 - \varepsilon_2(S_2^T)^{-1}\bar{W}_2^2] - \Gamma_2^{-1}\tilde{W}_2^T\dot{\hat{W}}_2 + S_2^T P_2 S_2 + S_2^T(t - \bar{T})P_2 S_2(t - \bar{T}).
\end{aligned}$$

(40)

For $\tilde{\omega}$, it is estimated by RBF neural network, that is,

$$\tilde{\omega}_i = \tilde{W}_i^T H_i(x), \; i = 1, 2.$$

(41)

Substituting equations (17),(19) and (41)into $\dot{V}_2$

$$\begin{aligned}
\dot{V}_2 =& S_1^T[-\beta_1 sat(S_1/\Delta_1) - A_1 S_1 - G_1 S_1(t - \bar{T}) + \tilde{W}_1^T(H_1(\hat{x}) + \varrho_1 I_{t1}) - \varepsilon_1(S_1^T)^{-1}\bar{W}_1^2] \\
&- \tilde{W}_1^T[S_1^T H_1(\hat{x}) + \mu_1\hat{W}_1 + \varrho_1 S_1^T I_{t1}] + S_1^T P_1 S_1 + S_1^T(t - \bar{T})P_1 S_1(t - \bar{T}) \\
&+ S_2^T[-\beta_2 sat(S_2/\Delta_2) - A_2 S_2 - G_2 S_2(t - \bar{T}) + \tilde{W}_2^T(H_2(\hat{x}) + \varrho_2 I_{t2}) - \varepsilon_2(S_2^T)^{-1}\bar{W}_2^2] \\
&- \tilde{W}_2^T[S_2^T H_2(\hat{x}) + \mu_2\hat{W}_2 + \varrho_2 S_2^T I_{t2}] + S_2^T P_2 S_2 + S_2^T(t - \bar{T})P_2 S_2(t - \bar{T}) \\
=& S_1^T[-\beta_1 sat(S_1/\Delta_1) - A_1 S_1] - S_1^T G_1 S_1(t - \bar{T}) - \varepsilon_1\bar{W}_1^2 - \mu_1\tilde{W}_1^T\hat{W}_1 + S_1^T P_1 S_1 \\
&+ S_1^T(t - \bar{T})P_1 S_1(t - \bar{T}) + S_2^T[-\beta_2 sat(S_2/\Delta_2) - A_2 S_2] - S_2^T G_2 S_2(t - \bar{T}) \\
&- \varepsilon_2\bar{W}_2^2 - \mu_2\tilde{W}_2^T\hat{W}_2 + S_2^T P_2 S_2 + S_2^T(t - \bar{T})P_2 S_2(t - \bar{T}).
\end{aligned}$$

(42)

Using Young's inequality, for $a, b \in R$, satisfying $ab \leq \frac{1}{2q}a^2 + \frac{1}{2q}b^2, (q > 0)$, we have:

$$-\mu_i\tilde{W}_i^T\hat{W}_i \leq -\frac{1}{2}\mu_i\tilde{W}_i^T\tilde{W}_i + \frac{1}{2}\mu_i\|W_i^*\|^2, \; i = 1, 2.$$

(43)

Similarly, for any y, z and positive definite symmetric matrix X, satisfying $-2z^T y \leq z^T X^{-1}z + y^T X y$,adopting Jensen integral inequality [22], we obtain:

$$-S_i^T G_i S_i(t - \bar{T}) \leq \frac{1}{2}S_i^T(t - \bar{T})G_i S_i(t - \bar{T}) + \frac{1}{2}S_i^T G_i S_i, \; i = 1, 2.$$

(44)

Substituting inequalities (43) and (44) into (42), we get:

$$
\begin{aligned}
\dot{V}_2 &\leq -\beta_1|S_1| - \beta_2|S_2| - S_1^T A_1 S_1 + \frac{1}{2}S_1^T(t-\bar{T})G_1 S_1(t-\bar{T}) + \frac{1}{2}S_1^T G_1 S_1 - \delta_1 \\
&\quad - \frac{1}{2}\mu_1 \tilde{W}_1^T \tilde{W}_1 + S_1^T P_1 S_1 + S_1^T(t-\bar{T})P_1 S_1(t-\bar{T}) - S_2^T A_2 S_2 + \frac{1}{2}S_2^T(t-\bar{T})G_2 S_2(t-\bar{T}) \\
&\quad + \frac{1}{2}S_2^T G_2 S_2 - \delta_2 - \frac{1}{2}\mu_2 \tilde{W}_2^T \tilde{W}_2 + S_2^T P_2 S_2 + S_2^T(t-\bar{T})P_2 S_2(t-\bar{T}) \\
&\leq -\beta_1|S_1| - \beta_2|S_2| - S_1^T(A_1 - P_1 - \frac{1}{2}G_1)S_1 - S_1^T(P_1 - \frac{1}{2}G_1)S_1(t-\bar{T}) - \delta_1 \\
&\quad - \frac{1}{2}\mu_1 \tilde{W}_1^T \tilde{W}_1 - S_2^T(A_2 - P_2 - \frac{1}{2}G_2)S_2 - S_2^T(P_2 - \frac{1}{2}G_2)S_2(t-\bar{T}) - \delta_2 - \frac{1}{2}\mu_2 \tilde{W}_2^T \tilde{W}_2
\end{aligned}
\tag{45}
$$

where $\delta_i = \varepsilon_i \bar{W}_i^2 - \frac{1}{2}\mu_i \|W_i^*\|^2$, $i = 1, 2$, because of $\|W^*\| \leq \bar{W}$, and $\varepsilon \geq \mu > 0$, it's clear that $\delta > 0$.

In order for the sliding surface to converge and the system to be globally stable and finally confined, from inequality (45) it is obvious that the designed gain matrix must satisfy the following inequality

$$
\begin{cases}
A_i - P_i - \frac{1}{2}G_i > 0 \\
P_i - \frac{1}{2}G_i > 0
\end{cases}
\quad i = 1, 2.
\tag{46}
$$

Therefore, considering inequality (44), when $V \geq 0$, we have $\dot{V} \leq 0$, then $S \in L_\infty$. Changing $\dot{S}$ to the intended control law τ:

$$
\dot{S}_i = -\beta_i sat(S_i/\Delta_i) - A_i S_i - G_i S_i(t-\bar{T}) + \tilde{\omega}_i - \varepsilon_i(S_i^T)^{-1}\bar{W}_i^2, \; i = 1, 2.
\tag{47}
$$

According to equation (47) and Lemma 3, we obtain $\dot{S} \in L_\infty$, that is, $t \to \infty$, $S \to 0$. Hence, the convergence of sliding surface with time-delay integral term is established. From equations (26) and (32), the virtual velocity tracking error e_u, e_v also converges. On the basis of Theorem 1, the position error x_e, y_e converges. The closed-loop system is hence uniformly globally stable and finally bounded.

5. SIMULATION

To verify how well the suggested ITDSMC tracks trajectories, the uncertainty of model parameters and the robustness of the system with input delays, the USV model is simulated by using MATLAB. The USV parameters considered in the simulation are as follows[15]: $m_{11} = 100kg, m_{22} = 80kg, m_{33} = 120kg, I_z = 50kg \cdot m^2, X_{\dot{u}} = -30kg, Y_{\dot{v}} = -80kg, N_{\dot{r}} = -30kg, X_u = 70kg/s, X_{u|u|} = 100kg/s, Y_v = 100kg/m, Y_{v|v|} = 200kg/m, N_r = 50kg \cdot m^2/s, N_{r|r|} = 100kg \cdot m^2/s$. In addition, this paper assumes that input delay is 0.5 s. In practice, USVs typically operate in complex environment. Therefore, 0.52 s is the time delay's maximum bound. In order to simulate the uncertainty of hydrodynamic coefficients of underactuated surface ships, a parametric disturbance of 10% is added to each nominal hydrodynamic coefficient. $\tau_{\omega u} = 3\sin(0.4t)N, \tau_{\omega v} = 1.2\cos(0.3t)N, \tau_{\omega r} = 4\sin(0.25t)N$. The radial basis function neural network has 31 hidden nodes, all the initial weights are selected as zero, the width of the basis function $b_1 = 5, b_2 = 2, b_3 = 4$, and the Gaussian function of the center point is evenly distributed between $[-8, 8]$.
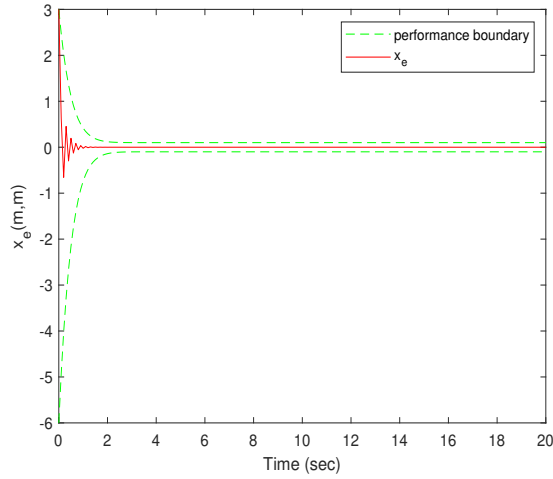
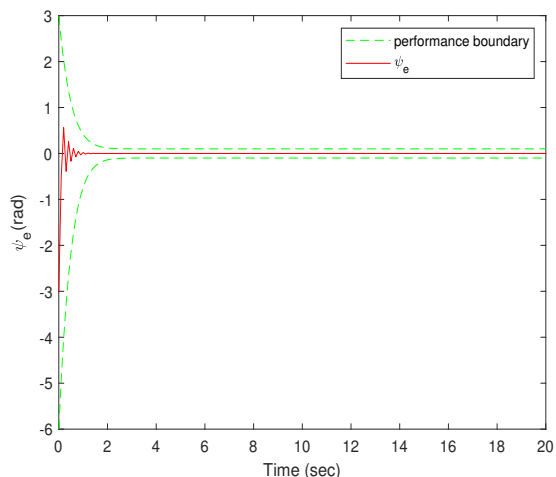**Fig. 4.** Position tracking error x_e with time delays.
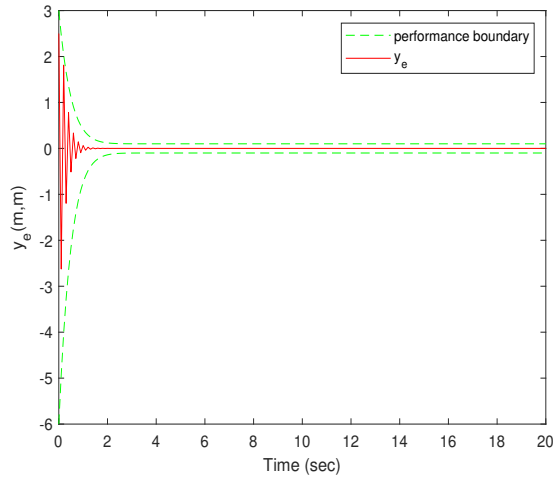
Fig. 5. Position tracking error y_e with time delays.

Figures 4 through 10 illustrate the simulation findings.

Figure 4, Figure 5 and Figure 6 are the curves of position tracking error and virtual velocity tracking error respectively under circumstance of input delays. Considering that the initial state value of the system is: $x_0 = 3, y_0 = 2.5, \psi_0 = -3rad$, and the control parameters are: $\beta_1 = 4 \times 10^{-3}, \beta_2 = 5 \times 10^{-3}, A_1 = 3.94 \times 10^{-2}, A_2 = 3.1475 \times 10^{-2}, G_1 =$

$1.5 \times 10^{-4}, G_2 = 1.5 \times 10^{-4}, \varepsilon = 5 \times 10^{-2}$. Meanwhile, setting the performance function parameters as follows: $\bar{e}_{1,0} = \bar{e}_{2,0} = 3, \underline{e}_{1,0} = \underline{e}_{2,0} = 6, \bar{e}_{i,t_f} = \underline{e}_{i,t_f} = 0.1, \ i = 1, 2, t_f = 10$. The simulation results of the application of the integral sliding mode control law demonstrate that the position error quickly converges to the performance function, and the error in virtual velocity tracking can react quickly to track the intended location. Meanwhile, it is obvious that the position tracking error of USV enters and no longer exceeds the preset steady-state error band when $t_f < 10s$. After 20 s, the USV achieved the control goal of tracking the desired trajectory. Although the virtual velocity error of USV converges to 0, the position tracking error oscillates during fast response and cannot converge smoothly to the origin.


Fig. 6. Position tracking error ψ_e with time delays.

It can be seen from Figure 7 that the response curves of control force and torque gradually smooth after 20 s, in line with the needs of practical engineering. In fact, the time delay of the real actuator is very small, but ignoring the delay to design the controller can lead to severe oscillations.
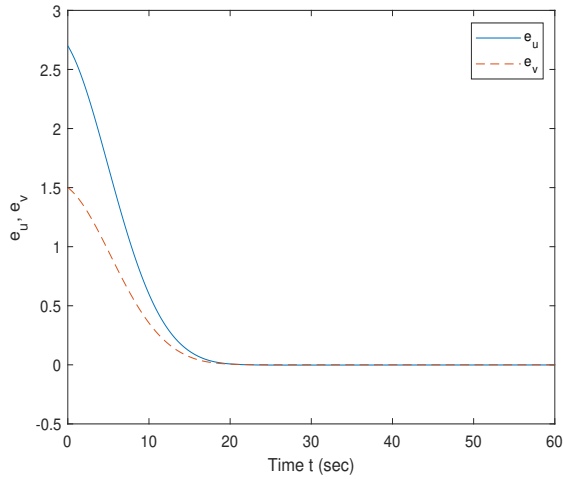
**Fig. 7.** Velocity tracking error with time delays.
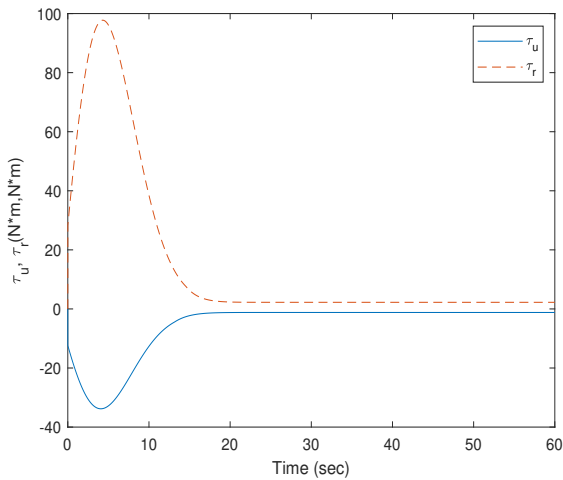
Fig. 8. Control input force and moment with time delays.

Figure 9 and Figure 10 show the error curve of RBF neural network's estimation of the composite disturbance terms ω_1, ω_2. As can be seen from figures, the estimated curve almost coincides with the actual disturbance curve, and the estimation error is small, indicating that the designed RBF neural network algorithm has a excellent estimation effect on composite disturbance.
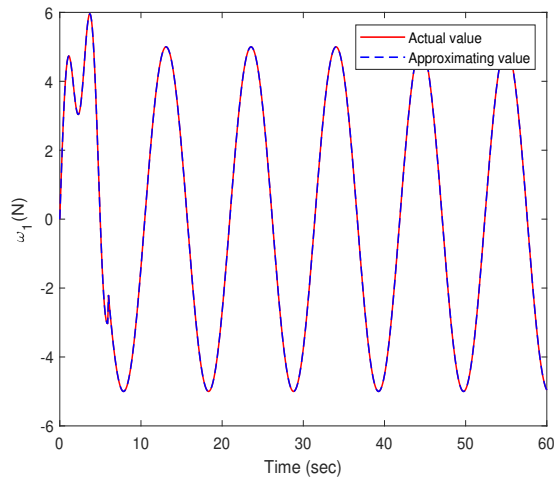
Fig. 9. Estimation curve of composite disturbance term ω_1 by RBF neural network
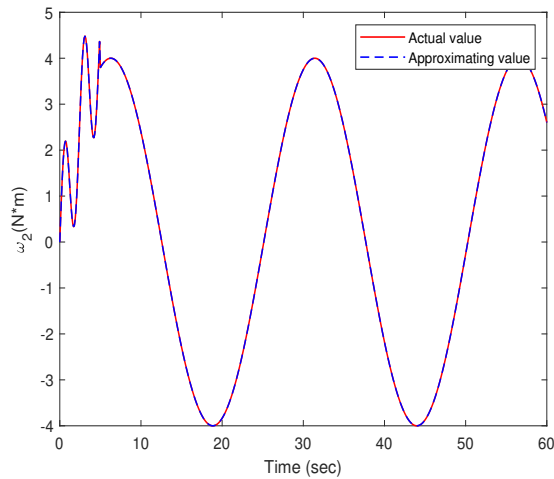
Fig. 10. Estimation curve of composite disturbance term ω_2 by RBF neural network.

6. CONCLUSION

The trajectory tracking for the USV with time delays and composite disturbances is addressed in this work using an backstepping-based integral time-delay sliding mode controller. Firstly, the virtual velocity control law is constructed utilizing coordinate

transformation and the backstepping approach to stabilize the position tracking error. Then, in order to counteract the effects of the disturbance on the system, the RBF neural network is built to estimate the nonlinear term with composite disturbances. For stabilizing the virtual velocity tracking error, the longitudinal control law and the yaw control law are built using the integral time-delay sliding mode approach. The stability theory and Lyapunov–Krasovskii functional serve as a foundation for the controller's assured resilience and convergence. The simulation results demonstrate that, if the assumptions are met, the controller proposed in this study is successful in achieving the control aim of trajectory tracking.

7. ACKNOWLEDGEMENTS

REFERENCES

[1] J. P. J. Avila, D. C. Donha, and J. C. Ad Amowski: Experimental model identification of open-frame underwater vehicles. Ocean Engrg. *60* (2013), 81–94. DOI:10.1016/j.oceaneng.2012.10.007

[2] S. Behtash: Robust output tracking for non-linear systems. Int. J. Control *51* (1990), 6, 1381–1407. DOI:10.1080/00207179008934141

[3] H. Chen, Y. Chen, and M. Wang: Trajectory tracking for underactuated surface vessels with time delays and unknown control directions. IET Control Theory Appl. *16* (2022), 6, 587–599. DOI:10.1049/cth2.12250

[4] W. Chen, Y. Wei, J. Zeng, J. Hu, and Z. Wang: Adaptive backstepping control of underactuated AUV based on disturbance observer. J. Central South University *48* (2017), 1, 69–76.

[5] Z. Chu, D. Zhu, S. X. Yang, G. E. and Jan: Adaptive Sliding mode control for depth trajectory tracking of remotely operated vehicle with thruster nonlinearity. J. Navigation *70* (2017), 1, 149–164. DOI:10.1017/S0373463316000448

[6] O. Druzhinina and N. Sedova: Optimization Problems in tracking control design for an underactuated ship with feedback delay, state and control constraints. Optim. Appl. *12422* (2020), 71–85. DOI:10.1007/978-3-030-62867-3_6

[7] J. Du and J. Li: Finite-time prescribed performance control for the three-dimension trajectory tracking of underactuated autonomous underwater vehicles. Control Theory Appl. *39* (2022), 383–392. DOI:0.1002/rnc.3106

[8] Z. Feng, J. Lam, and G.-H. Yang: Optimal partitioning method for stability analysis of continuous/discrete delay systems. Int. J. Robust Nonlinear Control *25* (2015), 4, 559–574. DOI:10.1002/rnc.3106

[9] Z. Jia, Z. Hu, and W. Zhang: Adaptive output-feedback control with prescribed performance for trajectory tracking of underactuated surface vessels. ISA Trans. *95* (2019), 18–56. DOI:10.1016/j.isatra.2019.04.035

[10] X. Jian, W. Man, and Q. Lei: Dynamical sliding mode control for the trajectory tracking of underactuated unmanned underwater vehicles. Ocean Engrg. *105* (2015), 54–63. DOI:10.1016/j.oceaneng.2015.06.022

[11] G. V. Lakhekar and L. M. Waghmare: Adaptive fuzzy exponential terminal sliding mode controller design for nonlinear trajectory tracking control of autonomous underwater vehicle. Int. J. Dynamics Control *6.4* (2018), 1690–1705. DOI:10.1007/s40435-017-0387-6

[12] Z. Y. Liao, Y. S. Dai, L. G. Li, J. C. Jin, F. and Shao: Overview of unmanned surface vehicle motion control methods. Marine Sci. *44* (2020), 3, 153–162.

[13] Y. L. Liao, M. J. Zhang, L. Wan, and Y. Li: Trajectory tracking control for underactuated unmanned surface vehicles with dynamic uncertainties. J. Central South Univ. *23* (2016), 2, 370–378. DOI:10.1007/s11771-016-3082-4

[14] Z. Liu: Practical backstepping control for underactuated ship path following associated with disturbances. IET Intell. Transport Systems *13* (2018), 5, 834–840. DOI:10.1049/iet-its.2018.5448

[15] J. E. Manley: Unmanned surface vehicles, 15 years of development. Oceans (2008), Supplement, 1–4.

[16] B. Marco, C. Massimo, and L. Lionel: Path-following algorithms and experiments for an autonomous surface vehicle. IFAC Proc. Vol. *40* (2007), 17, 81–86. DOI:10.3182/20070919-3-HR-3904.00015

[17] Y. Min and Y. Liu: Barbalat Lemma and its application in analysis of system stability. J. Shandong Univ., Engrg. Sci. (2007), 51–55+114. DOI:10.1002/rob.20353

[18] T. Pastore and V. Djapic: Improving autonomy and control of autonomous surface vehicles in port protection and mine countermeasure scenarios. J. Field Robotics *27* (2010), 6, 903–914. DOI:10.1002/rob.20353

[19] Y. Qijia: Robust fixed-time trajectory tracking control of marine surface vessel with feedforward disturbance compensation. Int. J. Systems Sci. *53* (2022), 4, 726–742. DOI:10.1080/00207721.2021.1972354

[20] B. Qiu, G. Wang, Y. Fan, D. Mu, and X. Sun: Adaptive sliding mode trajectory tracking control for unmanned surface vehicle with modeling uncertainties and input saturation. Appl. Sci. *9* (2019), 6, 1240. DOI:10.3390/app9061240

[21] K. Qudrat and A. Rini: Neuro-adaptive dynamic integral sliding mode control design with output differentiation observer for uncertain higher order MIMO nonlinear systems. Neurocomputing *226* (2017), 126–134. DOI:10.1016/j.neucom.2016.11.037

[22] K. Ramakrishnan, and G. Ray: Delay-range-dependent stability criterion for interval time-delay systems with nonlinear perturbations International Journal of Automation and Computing, vol.8.1, (2011), 141–146.

[23] F. Wang, Z. Chao, and L. Huang: Trajectory tracking control of robot manipulator based on RBF neural network and fuzzy sliding mode. Cluster Comput. *22* (2019), 3, 5799–5809. DOI:10.1007/s10586-017-1538-4

[24] D. Xu, Z. Liu, X. Zhou, L. Yang, and L. Huang: Trajectory tracking of underactuated unmanned surface vessels: non-singular terminal sliding control with nonlinear disturbance observer. Appl. Sci. *12* (2022), 6, 3004. DOI:10.3390/app12063004

[25] L. Yu, Z. Guoqing, Q. Lei, and Z. Weidong: Adaptive output-feedback formation control for underactuated surface vessels. Int. J. Control *93* (2020), 3, 400–409. DOI:10.1080/00207179.2018.1471221

[26] J. Zhou, Z. Xinyi, F. Zhiguang, and W. Di: Trajectory tracking sliding mode control for underactuated autonomous underwater vehicles with time delays. Int. J. Advanced Robotic Systems *17* (2020), 3, 1729881420916276. DOI:10.1177/1729881420916276

[27] J. Zhou, X. Zhao, T. Chen, Z. Yan, and Z. Yang: Trajectory tracking control of an underactuated AUV based on backstepping sliding mode with state prediction. IEEE Access *7* (2019), 181983–181993. DOI:10.1109/ACCESS.2019.2958360

[28] L. Zou, H. Liu, and X. Tian: Robust neural network trajectory-tracking control of underactuated surface vehicles considering uncertainties and unmeasurable velocities. IEEE Access*9* (2021), 117629–117638. DOI:10.1109/ACCESS.2021.3107033

Yun Chen, College of Mechanical and Electrical Engineering, Hohai University, No. 200, Jinling North Road, Changzhou, 213000. P. R. China.
  e-mail: 1435809002@qq.com

Hua Chen, Corresponding author. College of Science, Hohai University, No. 8, Focheng West Road, Nanjing, 210000. P. R. China.
  e-mail: chenhua112@163.com